PROCEEDINGS A

rspa.royalsocietypublishing.org

Research

Cite this article: Sharma AK, Arora N, Joglekar MM. 2018 DC dynamic pull-in instability of a dielectric elastomer balloon: an energy-based approach. *Proc. R. Soc. A* **474**: 20170900.
http://dx.doi.org/10.1098/rspa.2017.0900

Received: 25 December 2017
Accepted: 27 February 2018

Subject Areas:
mechanical engineering

Keywords:
dielectric elastomer, energy technique, dynamic instability, hyperelastic models

Author for correspondence:
M. M. Joglekar
e-mail: joglekarmm@yahoo.com

DC dynamic pull-in instability of a dielectric elastomer balloon: an energy-based approach

Atul Kumar Sharma, Nitesh Arora and M. M. Joglekar

Department of Mechanical and Industrial Engineering, Indian Institute of Technology Roorkee, Roorkee 247667, India

AKS, 0000-0001-9086-8441; NA, 0000-0003-2301-4264; MMJ, 0000-0003-0525-3923

This paper reports an energy-based method for the dynamic pull-in instability analysis of a spherical dielectric elastomer (DE) balloon subjected to a quasi-statically applied inflation pressure and a Heaviside step voltage across the balloon wall. The proposed technique relies on establishing the energy balance at the point of maximum stretch in an oscillation cycle, followed by the imposition of an instability condition for extracting the threshold parameters. The material models of the Ogden family are employed for describing the hyperelasticity of the balloon. The accuracy of the critical dynamic pull-in parameters is established by examining the saddle-node bifurcation in the transient response of the balloon obtained by integrating numerically the equation of motion, derived using the Euler–Lagrange equation. The parametric study brings out the effect of inflation pressure on the onset of the pull-in instability in the DE balloon. A quantitative comparison between the static and dynamic pull-in parameters at four different levels of the inflation pressure is presented. The results indicate that the dynamic pull-in instability gets triggered at electric fields that are lower than those corresponding to the static instability. The results of the present investigation can find potential use in the design and development of the balloon actuators subjected to transient loading. The method developed is versatile and can be used in the dynamic instability analysis of other conservative systems of interest.

THE ROYAL SOCIETY PUBLISHING

1. Introduction

The nonlinear behaviour of a spherical elastomeric balloon during inflation, in particular, the non-monotonic behaviour of inflation pressure as a function of the balloon volume and the associated problem of bifurcation and 'snap-through' instability, have been well known for many years. Since the early 1970s, after Alexander's [1] seminal experimental work based on the hypothesis proposed by Green & Adkins [2], a large volume of theoretical studies have been conducted on this subject [3–7].

Dielectric elastomers (DEs), electro-active polymer (EAP) capable of producing large strain when subjected to stimulus of combined mechanical and electrical loading, have gained increasing attention in the recent past [8]. Owing to their peculiar properties, such as fast response, light weight, low cost, high energy density and large voltage-induced deformation, these materials are being explored intensively in the development of electromechanical transducers. [9]. The typical architectures of these devices comprise a DE membrane sandwiched between a pair of compliant electrodes. Subject to a potential difference through the thickness, the elastomeric membrane reduces in thickness and expands in surface area [10]. It has been reported that the areal strain may reach well beyond 100% before breakdown [8,9]. The DE actuators (DEAs) are susceptible to a phenomena called electromechanical instability or pull-in instability when actuated electrostatically. Physically, when the voltage increases, the DE membrane thins down, and the same voltage leads to a higher electric field. Because of this positive feedback, the DE membrane thins down catastrophically and finally fails by electrical breakdown [11,12]. The pull-in instability parameters, i.e. electric field and corresponding actuation stretch strongly depend on the material model and on the other several factors, such as temperature, material permittivity and prestress [13–16].

The particular configuration of a spherical balloon made from dielectric material is especially interesting for the soft generators and actuators [17,18]. In this regard, Ahmadi *et al.* [19] presented a method for fabricating and testing a spherical DE balloon. In the past, electromechanical behaviour and electromechanical instability of the spherical DE balloon, when subjected to quasi-statically applied voltage has been extensively studied theoretically as well as experimentally [20–26]. Rudykh *et al.* [20] studied the static actuation of a thick-walled electroactive balloon for different material models and inferred that electromechanical instability is affected by both boundary conditions and material models. Xie *et al.* [22] studied the shape bifurcation of ideal and non-ideal DE balloons under pressurized inflation and electric voltage. Sun *et al.* [27] investigated the actuation and instability of interconnected DE balloons.

However, relatively few researchers have addressed the dynamic performance of the DEAs, specifically for the spherical shape balloon actuators. Zhu *et al.* [28] studied the dynamic electromechanical behaviour of a thin spherical balloon made from the DE, when subjected to a constant internal pressure and an AC voltage. For investigating the dynamic response of a thick spherical shell made of soft dielectric membrane, an explicit equation of motion was developed analytically by Yong *et al.* [29]. Mockensturm *et al.* [30] studied the dynamic behaviour of a spherical DE shell under pressure in which electric effects were accounted for through a body force term. Chen *et al.* [31] studied the dynamic performance of a DE balloon actuator when driven by high internal pressure of air inside and the periodic electric voltage signal. The nonlinear oscillation of a thin circular DE membrane when subjected to combined mechanical and electrical loading was investigated by Zhu *et al.* [32] who inferred that variation in the prestretch, pressure and voltage may be used for tuning the natural frequency of the membrane. The effects of several factors such as prestress [16], initial stretch ratio [33], viscoelasticity [34,35] and a combined DC and AC voltage [36] on the electromechanical performance of the DE transducers have been reported in the literature in the recent past. Liu *et al.* [37] investigated the effect of viscoelasticity on the nonlinear dynamics of a DE balloon using the shooting and arc-length continuation method. In view of the potential applications of the spherical DE balloons in reciprocating or peristaltic pumps [38], tactile devices [39], acoustic actuators [40], soft loudspeakers [41] that

innately involve a dynamic motion, it is necessary to study pull-in instability of the DE balloon actuators in a dynamic mode of actuation.

In this connection, Chen *et al.* [31] reported a method which is based on time-integration of the equation of motion of the DE balloons for investigating dynamic electromechanical instability. With reference to planar DEAs, Xu *et al.* [42] also suggested the same approach for pull-in instability analysis in the dynamic mode of operation and inferred that the dynamic pull-in instability can be set at an electric field remarkably lower than that in the quasi-static mode of operation. This was followed by Joglekar [43,44], who proposed an energy-based method for excerpting the instability parameters of a planar DEA in the dynamic mode considering the effect of prestress. To the best of our knowledge, the effect of pre-inflation pressure on the dynamic pull-in instability parameters of a DE balloon has not been yet reported. To this end, the main aim of this paper is to report an energy-based technique for excerpting the instability parameters of a spherical DE balloon with different levels of inflation pressure, in the static and dynamic modes of operations. This energy method eludes the iterative process of performing time integration of the equation of motion for obtaining the dynamic pull-in instability parameters [42] and is based on setting the energy balance at the stagnation point in the oscillation cycles followed by the imposition of the condition of instability. A parametric study is performed for estimating the effect of pre-inflation pressure on the instability parameters of the DE balloon for three widely used material models, i.e. neo-Hookean, Mooney–Rivlin and Ogden models. The pull-in instability estimates in the dynamic mode of operation for each material model are concurred by numerically integrating the equation of motion of the DE balloon.

The rest of this article is organized into four sections as follows. In the following §2, after defining the problem statement, we discuss the material modelling of an ideal DE. In §3, we present an energy-based method for estimating the pull-in instability parameters of a DE balloon for two-parameter Ogden model. To corroborate the dynamic pull-in instability parameters, the equation of motion is developed using the Euler–Lagrange equation. In §4, static and dynamic pull-in instability parameters are presented for different inflation pressure levels in the balloon for three material models of interest. Various trends obtained in the parametric study are presented and discussed. Eventually, the paper concludes with a summary of salient inferences, in §5.

2. Problem definition and material model

Figure 1 illustrates the schematic of the problem of interest, an electrostatically actuated spherical DE balloon sandwiched by compliant electrodes on its two surfaces. In the reference configuration, the balloon is of radius R and thickness H and subjected to a constant inflation pressure and a voltage. Each material point of the membrane is denoted by the radius R, as shown in figure 1*a*. Under the action of a constant net pressure p inside the balloon and the electrostatic force developed through a time-varying potential difference $\phi(t)$, the dielectric membrane reduces its thickness, while the balloon expands proportionately in surface area and the two electrodes gain electric charge of magnitude Q. In the present investigation, the DE balloon is assumed to be thin-walled and the electric field, developed because of applied voltage, along the thickness of the membrane is assumed to be homogeneous throughout the deformation. At the moment t, the DE balloon is of radius r and thickness h in the current configuration as shown in figure 1*b*. Let the deformation field of the balloon is defined by the hoop stretch λ, as

$$\lambda = \frac{r}{R}. \tag{2.1}$$

The hoop stretch λ is a function of time t only, i.e. $\lambda = \lambda(t)$. An isothermal condition is assumed in the present analysis, and hence, no temperature change will be considered explicitly. The balloon is assumed to be made of isotropic and incompressible hyperelastic material, so that

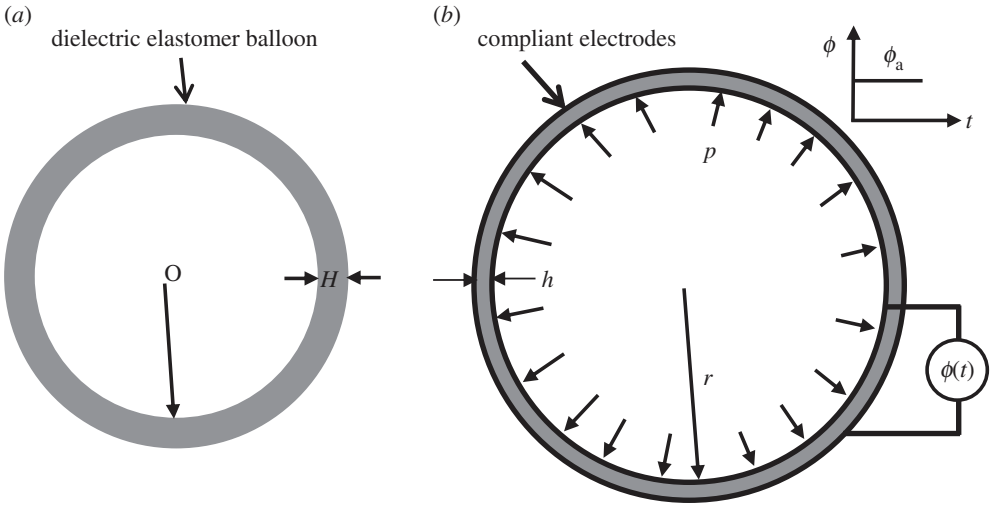

Figure 1. Schematic of a spherical DE balloon, sandwiched between two compliant electrodes, subjected to inflation pressure (p) and step voltage (ϕ_a), in the (a) reference configuration and (b) current configuration.

$4\pi R^2 H = 4\pi r(t)^2 h(t)$; the thickness of the balloon in the current configuration $h(t)$ is expressed in terms of hoop stretch as follows:

$$h = \frac{H}{\lambda(t)^2}. \tag{2.2}$$

The true electric field E in the thickness direction of the balloon is defined as the applied voltage (ϕ_a) divided by the balloon thickness in the current state ($h(t)$), as

$$E = \frac{\phi_a}{h(t)} = \frac{\phi_a \lambda^2}{H} \tag{2.3}$$

and the true electric displacement D is defined as the charge on the electrode divided by the surface area of the electrode in the current state, as

$$D = \frac{Q}{4\pi (r(t))^2} = \frac{Q}{4\pi R^2 \lambda^2}. \tag{2.4}$$

To model the electromechanical behaviour of the balloon membrane, we adopted the constitutive model of an ideal DE, which assumes the dielectric behaviour to be independent of deformation [11]. The true electric field E has a linear relation with the true electric displacement D as

$$D = \varepsilon E, \tag{2.5}$$

in which ε is the permittivity of the balloon membrane, which is assumed to be constant throughout the deformation. Thus, the thermodynamics of an ideal DE balloon is characterized by the Helmholtz free-energy density function $\psi(\lambda, D)$ written as

$$\psi(\lambda, D) = \psi_m(\lambda) - \frac{D^2}{2\varepsilon}, \tag{2.6}$$

where ψ_m is the elastic energy density of the elastomer in the deformed state, for which we widely used the Ogden family of hyperelastic material models, i.e. Ogden, Mooney–Rivlin and

neo-Hookean models are used to describe the hyperelasticity of balloon membrane. Based on the Ogden model [45], the strain energy density of the incompressible elastomer balloon is written as

$$\psi_m = \sum_{r=1}^{n} \frac{\mu_r}{\alpha_r}\left(2\lambda^{\alpha_r} + \frac{1}{\lambda^{2\alpha_r}} - 3\right), \tag{2.7}$$

where α_r and μ_r are material constants. To be specific, the analysis in this paper is restricted to the two-parameter Ogden model ($n=2$), Mooney–Rivlin model ($n=2, \alpha_1=2, \alpha_2=-2$) and single-parameter neo-Hookean model ($n=1, \alpha_1=2$). However, the analysis can be extended to higher values of constant n. Taking ($n=2$), the expression for the elastic energy density of the balloon in the deformed state is written as

$$\psi_m = \frac{\mu_1}{\alpha_1}\left[\left(2\lambda^{\alpha_1} + \frac{1}{\lambda^{2\alpha_1}} - 3\right) + \xi\left(2\lambda^{\alpha_2} + \frac{1}{\lambda^{2\alpha_2}} - 3\right)\right], \tag{2.8}$$

where ξ is a material constant written as $\xi = \mu_2\alpha_1/\mu_1\alpha_2$. On substituting the expression of true electric field E from equation (2.3) into equation (2.5), and on inheriting the resulting expression of true electric displacement D and elastic energy density ψ_m from equation (2.8), the Helmholtz free-energy density ψ of the balloon is expressed as

$$\psi = \left[\frac{\mu_1}{\alpha_1}\left\{2\lambda^{\alpha_1} + \frac{1}{\lambda^{2\alpha_1}} - 3 + \xi\left(2\lambda^{\alpha_2} + \frac{1}{\lambda^{2\alpha_2}} - 3\right)\right\} - \frac{1}{2}\varepsilon\tilde{E}^2\lambda^4\right], \tag{2.9}$$

where $\tilde{E} = \phi_a/H$ is the electric field in the reference configuration with ϕ_a being the applied potential difference.

The DE balloon experiences an electromechanical instability or pull-in instability at the critical value of applied voltage. If the applied voltage is further increased beyond its critical value, an uncontrolled reduction in the thickness occurs and the balloon actuator ultimately undergoes failure because of dielectric breakdown [42,46]. In the upcoming section, a computationally efficient energy-based technique is presented for estimating the pull-in instability parameters of the DE balloon in both the dynamic and static modes of actuation.

3. Solution method

This section presents an energy-based method with an intent to estimate the pull-in instability parameters of a DE balloon actuator. First of all, we outline the proposed energy approach for extracting the static and dynamic pull-in instability parameters of a DE balloon with a two-parameter Ogden model. Subsequently, the equation of motion of the DE balloon is developed using the Euler–Lagrange equation for corroborating the dynamic pull-in instability parameters.

(a) Extraction of static pull-in instability parameters

In the following discussion, we consider that a spherical elastomer balloon is first inflated quasi-statically. As the inflation pressure increases, the balloon slowly expands homogeneously until a critical pressure is reached. The elastomeric balloon experiences snap-through instability if the inflation pressure exceeds the limiting value. The critical internal pressure and corresponding critical stretch are first estimated using the principle of stationary total potential energy.

The total strain or elastic energy of the DE balloon in the deformed or current state is obtained by the integral of the strain energy density function (ψ_m) in equation (2.8) over the volume of the balloon and takes the form

$$W_s = \int_V \psi_m \, \mathrm{d}V = \frac{4\pi R^2 H \mu_1}{\alpha_1}\left[\left(2\lambda^{\alpha_1} + \frac{1}{\lambda^{2\alpha_1}} - 3\right) + \xi\left(2\lambda^{\alpha_2} + \frac{1}{\lambda^{2\alpha_2}} - 3\right)\right], \tag{3.1}$$

where V is the volume of the balloon.

The work done by the internal pressure p is obtained by integrating the elemental work done $\mathrm{d}W_\mathrm{p} = 4\pi r^2 p\,\mathrm{d}r$ over the whole elastomer as

$$W_\mathrm{p} = -4\pi p\int_R^r r^2\,\mathrm{d}r = -\frac{4\pi}{3}p(r^3 - R^3) = -\frac{4\pi}{3}pR^3(\lambda^3 - 1). \tag{3.2}$$

The total potential energy U_p of the DE balloon in the pressurized state is expressed using equations (3.1)–(3.2) as

$$U_\mathrm{p} = 4\pi R^2 H\left[\frac{\mu_1}{\alpha_1}\left\{2\lambda_\mathrm{p}^{\alpha_1} + \frac{1}{\lambda_\mathrm{p}^{2\alpha_1}} - 3 + \xi\left(2\lambda_\mathrm{p}^{\alpha_2} + \frac{1}{\lambda_\mathrm{p}^{2\alpha_2}} - 3\right)\right\} - \frac{pR(\lambda_\mathrm{p}^3 - 1)}{3H}\right], \tag{3.3}$$

where λ_p is the hoop stretch that arises because of applied internal pressure p. Setting the first derivative of the total potential energy in equation (3.3) with respect to λ_p equal to zero, i.e. $\mathrm{d}U_\mathrm{p}/\mathrm{d}\lambda_\mathrm{p} = 0$, the numerical value of hoop stretch λ_p can be extracted for any level of internal pressure p and for given material parameters by solving the equilibrium equation expressed as

$$\gamma = 2\left(\lambda_\mathrm{p}^{\alpha_1 - 3} - \frac{1}{\lambda_\mathrm{p}^{2\alpha_1 + 3}}\right) + \frac{2\alpha_2\xi}{\alpha_1}\left(\lambda_\mathrm{p}^{\alpha_2 - 3} - \frac{1}{\lambda_\mathrm{p}^{2\alpha_2 + 3}}\right). \tag{3.4}$$

The dimensionless inflation pressure stated in equation (3.4) is defined as $\gamma = pR/\mu_1 H$. To estimate the critical inflation pressure and corresponding stretch, the condition of instability, i.e. $\mathrm{d}\gamma/\mathrm{d}\lambda_\mathrm{p} = 0$ is applied, which yields the following nonlinear equation:

$$(\alpha_1 - 3)\lambda_\mathrm{p}^{\alpha_1} + \frac{(2\alpha_1 + 3)}{\lambda_\mathrm{p}^{2\alpha_1}} + \frac{\alpha_2\xi}{\alpha_1}\left((\alpha_2 - 3)\lambda_\mathrm{p}^{\alpha_2} + \frac{(2\alpha_2 + 3)}{\lambda_\mathrm{p}^{2\alpha_2}}\right) = 0. \tag{3.5}$$

The solution of equation (3.5) along with equation (3.4) for dimensionless pressure γ and λ_p yields the critical inflation pressure and hoop stretch represented by γ^c and $\lambda_\mathrm{p}^\mathrm{c}$, respectively.

The DE balloon, with internal pressure below its critical value estimated in the aforementioned discussion, experiences the electromechanical or pull-in instability when the electric field applied across its wall exceeds a critical value [27,28,31]. Here, we present an energy approach for obtaining the pull-in instability parameters (critical actuation stretch and critical electric field) of a pre-inflated DE balloon, when potential difference ϕ across the balloon wall is applied quasi-statically.

The total potential energy of a pre-inflated DE balloon actuator under the quasi-static mode of actuation is obtained as

$$\begin{aligned} U &= \int_V \psi(\lambda, \tilde{E})\,\mathrm{d}V + W_\mathrm{p} \\ &= 4\pi R^2 H\left[\frac{\mu_1}{\alpha_1}\left\{2\lambda^{\alpha_1} + \frac{1}{\lambda^{2\alpha_1}} - 3 + \xi\left(2\lambda^{\alpha_2} + \frac{1}{\lambda^{2\alpha_2}} - 3\right)\right\} - \frac{1}{2}\varepsilon\tilde{E}^2\lambda^4 - \frac{pR(\lambda^3 - 1)}{3H}\right]. \end{aligned} \tag{3.6}$$

In the non-dimensional form, the expression for the total potential energy of the balloon actuator is written as

$$\hat{U} = \left[\frac{1}{\alpha_1}\left\{2\lambda^{\alpha_1} + \frac{1}{\lambda^{2\alpha_1}} - 3 + \xi\left(2\lambda^{\alpha_2} + \frac{1}{\lambda^{2\alpha_2}} - 3\right)\right\} - \frac{1}{2}e^2\lambda^4 - \frac{1}{3}\gamma(\lambda^3 - 1)\right], \tag{3.7}$$

in which, $\hat{U} = U/4\pi R^2 H\mu_1$ is the dimensionless total potential energy of the balloon in the actuated state, while $e = \tilde{E}\sqrt{\varepsilon/\mu_1}$ is the non-dimensional nominal electric field. The static pull-in instability parameters of the DE balloon are extracted by setting the first two derivatives of the dimensionless total potential energy $\hat{U}$ with respect to hoop stretch λ equal to zero and solving

the resulting system of nonlinear algebraic equations for the dimensionless instability field e and hoop stretch λ. The resulting nonlinear algebraic equations are written as

$$\frac{\mathrm{d}\hat{U}}{\mathrm{d}\lambda}=0 \;\Rightarrow\; \alpha_1\left(\lambda^{\alpha_1}-\frac{1}{\lambda^{2\alpha_1}}\right)+\alpha_2\xi\left(\lambda^{\alpha_2}-\frac{1}{\lambda^{2\alpha_2}}\right)-\frac{\alpha_1\gamma\lambda^3}{2}-\alpha_1 e^2\lambda^4=0 \tag{3.8}$$

and

$$\frac{\mathrm{d}^2\hat{U}}{\mathrm{d}\lambda^2}=0 \;\Rightarrow\; \alpha_1^2\left(\lambda^{\alpha_1}+\frac{2}{\lambda^{2\alpha_1}}\right)+\alpha_2^2\xi\left(\lambda^{\alpha_2}+\frac{2}{\lambda^{2\alpha_2}}\right)-\frac{3\alpha_1\gamma\lambda^3}{2}-4\alpha_1 e^2\lambda^4=0. \tag{3.9}$$

The solution of nonlinear algebraic equations (3.8)–(3.9) for hoop stretch and dimensionless electric field results into the critical values denoted by λ_c^S, and e_c^S for any given value of dimensionless pressure γ and material constants. In the present work, the value of pre-inflation pressure is kept below its limiting value γ_c. The static instability actuation stretch (λ_{ac}^S) corresponding to these parameters is calculated as $\lambda_{ac}^S=\lambda_c^S/\lambda_p$. These dimensionless parameters e_c^s and λ_{ac}^S are collectively introduced as the static pull-in instability parameters. The stretch in the pressurized state λ_p can be calculated by solving nonlinear algebraic as stated in equation (3.4) for the known value of γ. The generalized nonlinear equations (3.8)–(3.9) stated for extracting the static instability parameters of the Ogden material model can be reduced to that corresponding to the Mooney–Rivlin model by substituting $\alpha_1=2$ and $\alpha_2=-2$ or the neo-Hookean model by substituting $\alpha_1=2$, $\alpha_2=0$ and $\xi=0$.

(b) Extraction of dynamic pull-in instability parameters

When the DE balloon is subjected to quasi-statically applied internal pressure and DC step voltage signal, the hoop stretch (λ) in the balloon shows the periodic response [28]. The planer DEAs show a similar periodic response observed experimentally when subjected to step voltage [47]. The amplitude and time period of the periodic response is dependent on the extent of applied step voltage signal [42]. The stretch in the balloon because of the applied step voltage overshoots, the hoop stretch arises due to the same magnitude of voltage when applied quasi-statically. When the overshoot in the hoop stretch because of the applied step voltage is sufficiently large, the DE balloon cannot regain its original state and the dielectric membrane can fail because of the dielectric breakdown [48]. The proposed energy technique of obtaining the pull-in instability parameters in the dynamic mode of actuation is based on the principle of energy conservation, which states that, at each and every state in the oscillation cycle, the electrostatically supplied energy will be equal to the sum of the kinetic and the potential energy of the DE balloon. Thus, upon setting up the energy balance between the electrostatic energy, elastic energy and kinetic energy, at the position of maximum actuation in an oscillation cycle, and invoking the Hamiltonian method, the equation of the stagnation state is obtained. For conservative systems, the Hamiltonian is the sum of total potential energy and the kinetic energy of the system and may be expressed as

$$\mathcal{H}=U+T, \tag{3.10}$$

where U is the total potential energy and T is the kinetic energy of a conservative balloon actuator.

The kinetic energy (T) of the DE balloon, neglecting the velocity components in the hoop direction of the balloon, is written as [37]

$$T=\frac{1}{2}mv^2=\frac{1}{2}\rho V\left(\frac{\partial r(t)}{\partial t}\right)^2=2\pi\rho R^4 H\left(\frac{\mathrm{d}\lambda}{\mathrm{d}t}\right)^2, \tag{3.11}$$

where ρ is the density of the DE material and assumed to be independent of deformation because of conservation of volume, v is the radial velocity of the balloon and m is the mass of balloon in

the deformed state. In the dimensionless form the kinetic energy is expressed as

$$\hat{T} = \frac{T}{4\pi R^2 H \mu_1} = \frac{\rho R^2}{2\mu_1}\left(\frac{\mathrm{d}\lambda}{\mathrm{d}t}\right)^2. \tag{3.12}$$

On inserting the expression of the dimensionless total potential energy from equation (3.7) and the dimensionless kinetic energy from equation (3.12) into equation (3.10), the non-dimensional form of the Hamiltonian of the balloon actuator is written in terms of hoop stretch λ and its time derivative $\mathrm{d}\lambda/\mathrm{d}t$ as follows:

$$\hat{\mathcal{H}}(t) = \left[\begin{array}{c} \dfrac{1}{\alpha_1}\left\{2\lambda^{\alpha_1} + \dfrac{1}{\lambda^{2\alpha_1}} - 3 + \xi\left(2\lambda^{\alpha_2} + \dfrac{1}{\lambda^{2\alpha_2}} - 3\right)\right\} \\ -\dfrac{1}{2}e^2\lambda^4 - \dfrac{1}{3}\gamma(\lambda^3 - 1) + \dfrac{\rho R^2}{2\mu_1}\left(\dfrac{\mathrm{d}\lambda}{\mathrm{d}t}\right)^2 \end{array}\right]. \tag{3.13}$$

In the present investigation, we assume that the actuator starts from rest with the two initial conditions given as

$$\lambda|_{t=0} = \lambda_\mathrm{p}; \quad \left.\frac{\mathrm{d}\lambda}{\mathrm{d}t}\right|_{t=0} = 0, \tag{3.14}$$

where λ denotes the stretch level in the balloon at the equilibrium state when subjected to inflation pressure p and is estimated by solving equilibrium equation stated in equation (3.4). The expression for initial dimensionless Hamiltonian $\mathcal{H}(0)$ of the DE balloon is obtained by using the two initial conditions expressed in equation (3.14) as follows:

$$\hat{\mathcal{H}}(0) = \left[\frac{1}{\alpha_1}\left\{2\lambda_\mathrm{p}^{\alpha_1} + \frac{1}{\lambda_\mathrm{p}^{2\alpha_1}} - 3 + \xi\left(2\lambda_\mathrm{p}^{\alpha_2} + \frac{1}{\lambda_\mathrm{p}^{2\alpha_2}} - 3\right)\right\} - \frac{1}{2}e^2\lambda_\mathrm{p}^4 - \frac{1}{3}\gamma(\lambda_\mathrm{p}^3 - 1)\right]. \tag{3.15}$$

As the actuator system under consideration is conservative and the Hamiltonian of the DE balloon will remain unchanged. We can equate the dimensionless Hamiltonian of the balloon $\hat{\mathcal{H}}(t)$ at a particular time t to the initial dimensionless Hamiltonian $\hat{\mathcal{H}}(0)$ as, $\hat{\mathcal{H}}(t) = \hat{\mathcal{H}}(0)$. This condition physically shows the energy balance between the electrostatic energy supplied to the actuator, kinetic energy and elastic energy of the DE balloon. Zero velocity of the actuator at the position of maximum deformation in an oscillation cycle will yield the zero dimensionless kinetic energy ($\hat{T}$) of the DE balloon actuator. Thus, the Hamiltonian in the non-dimensional form ($\hat{\mathcal{H}}$) can be equated to the dimensionless total potential energy ($\hat{U}$) of the balloon actuator. The expression for the Hamiltonian of the actuator in the non-dimensional form at the maximum overshoot point is obtained by setting ($\mathrm{d}\lambda/\mathrm{d}t$) to zero in equation (3.13) as

$$\hat{\mathcal{H}}(t) = \left[\frac{1}{\alpha_1}\left\{2\tilde{\lambda}^{\alpha_1} + \frac{1}{\tilde{\lambda}^{2\alpha_1}} + \xi\left(2\tilde{\lambda}^{\alpha_2} + \frac{1}{\tilde{\lambda}^{2\alpha_2}}\right)\right\} - \frac{1}{2}e^2\tilde{\lambda}^4 - \frac{1}{3}\gamma(\tilde{\lambda}^3 - 1)\right], \tag{3.16}$$

in which $\tilde{\lambda}$ is the hoop stretch at the position of maximum overshoot in the oscillations. On inserting the expression for $\hat{\mathcal{H}}(t)$ and $\hat{\mathcal{H}}(0)$ from equations (3.15) and (3.16) into the aforementioned energy constraint $\hat{\mathcal{D}} = \hat{\mathcal{H}}(t) - \hat{\mathcal{H}}(0) = 0$, the equation of the stagnation curve is obtained as

$$\hat{\mathcal{D}} = \left[\begin{array}{c} \dfrac{1}{\alpha_1}\left\{2(\tilde{\lambda}^{\alpha_1} - \lambda_\mathrm{p}^{\alpha_1}) + \dfrac{1}{\tilde{\lambda}^{2\alpha_1}} - \dfrac{1}{\lambda_\mathrm{p}^{2\alpha_1}} + \xi\left(2(\tilde{\lambda}^{\alpha_2} - \lambda_\mathrm{p}^{\alpha_2}) + \dfrac{1}{\tilde{\lambda}^{2\alpha_2}} - \dfrac{1}{\lambda_\mathrm{p}^{2\alpha_2}}\right)\right\} \\ -\dfrac{1}{2}e^2(\tilde{\lambda}^4 - \lambda_\mathrm{p}^4) - \dfrac{\gamma(\tilde{\lambda}^3 - \lambda_\mathrm{p}^3)}{3} \end{array}\right] = 0. \tag{3.17}$$

This equation of the stagnation state is only valid for all points of maximum overshoot caused by dimensionless electric field e that are equal to or below the electric field at the onset of pull-in instability in the dynamic mode of operation. This is followed by application of the condition of instability, i.e. $\partial\hat{\mathcal{D}}/\partial\tilde{\lambda} = 0$, to equation (3.17) for excerpting the pull-in instability hoop stretch and the corresponding electric field in the dynamic mode for any level of dimensionless pressure γ.

This yields the following nonlinear algebraic equation

$$\tilde{\lambda}^{\alpha_1} - \frac{1}{\tilde{\lambda}^{2\alpha_1}} + \frac{\alpha_2 \xi}{\alpha_1}\left(\tilde{\lambda}^{\alpha_2} - \frac{1}{\tilde{\lambda}^{2\alpha_2}}\right) - \frac{\gamma \tilde{\lambda}^3}{2} - e^2\tilde{\lambda}^4 = 0. \tag{3.18}$$

The solution of the system of nonlinear algebraic equations stated in equations (3.17)–(3.18) for two unknowns, electric field e and hoop stretch, $\tilde{\lambda}$, results into the critical parameters λ_c^D and e_c^D for known values of non-dimensional internal pressure γ. The critical actuation stretch λ_{ac}^D corresponding to these parameters is calculated as $\lambda_{ac}^D = \lambda_c^D/\lambda_p$. These parameters e_c^D and λ_{ac}^D are collectively introduced as pull-in instability parameters of the DE balloon in the dynamic mode of actuation.

(c) Extraction of dynamic pull-in instability parameters: numerical integration of the equation of motion

For corroborating the dynamic pull-in parameters of the DE balloon extracted using an energy-based technique discussed in the previous subsection, we construct the equation of motion of the DE balloon actuator. Based on the principle of least action, the non-dimensional form of the Euler–Lagrange equation is expressed as [49]:

$$\frac{\mathrm{d}}{\mathrm{d}t}\left(\frac{\partial \hat{\mathcal{L}}}{\partial \dot{\lambda}}\right) - \frac{\partial \hat{\mathcal{L}}}{\partial \lambda} = 0, \quad \text{where } \hat{\mathcal{L}} = \hat{T} - \hat{U}, \tag{3.19}$$

where $\dot{\lambda}$ is the time derivative of hoop stretch, i.e. $(\partial\lambda/\partial t)$, and $\hat{\mathcal{L}}$ is the difference between the non-dimensional kinetic energy ($\hat{T}$) and the non-dimensional total potential energy ($\hat{U}$) of the DE balloon.

On inheriting the non-dimensional kinetic energy ($\hat{T}$) expression from equation (3.12) and the non-dimensional total potential energy ($\hat{U}$) expression from equation (3.7) and inserting into equation (3.19), the resulting equation of motion of the balloon actuator in dimensionless form is written as

$$\frac{\mathrm{d}^2\lambda}{\mathrm{d}\tau^2} + 2\lambda^{\alpha_1 - 1} - \frac{2}{\lambda^{2\alpha_1+1}} + \frac{\alpha_2 \xi}{\alpha_1}\left(2\lambda^{\alpha_1-1} - \frac{2}{\lambda^{2\alpha_1+1}}\right) - \gamma\lambda^2 - 2e^2\lambda^3 = 0, \tag{3.20}$$

where $\tau = t\sqrt{\mu_1/\rho R^2}$ is the non-dimensional time. The ordinary differential equation stated in equation (3.20) shows that the dynamics of the DE balloon involves high nonlinearity, caused by the balloon geometry and the intrinsic material nonlinearity characterized by the Ogden model. Equation (3.20) recovers the equation of static equilibrium stated in equation (3.8) if the time-dependent terms are set equal to zero. The differential equation in equation (3.20) together with two initial conditions given in equation (3.14) is solved using MATLAB ODE solver for different levels of dimensionless pressure (γ) and non-dimensional electric field (e) for obtaining transient response of hoop stretch of the DE balloon. The response of the DE balloon actuator for the applied value of dimensionless electric field e below critical value is periodic for any given value of non-dimensional pressure. The least value of the applied field that distinguishes the periodic and aperiodic motion of the balloon is known as the electric field at the onset of dynamic pull-in instability [42,50,51]. On further increment in the applied electric field, the DE balloon finally fails because of dielectric breakdown [44].

In the following section, the effect of pre-inflation pressure on the static and dynamic pull-in instability parameters of a spherical DE balloon made up of three material models of interest is investigated.

4. Results and discussion

In the following, the effect of pre-inflation pressure on the static and dynamic pull-in instability parameters of a DE balloon actuator is studied on the basis of the energy approach outlined

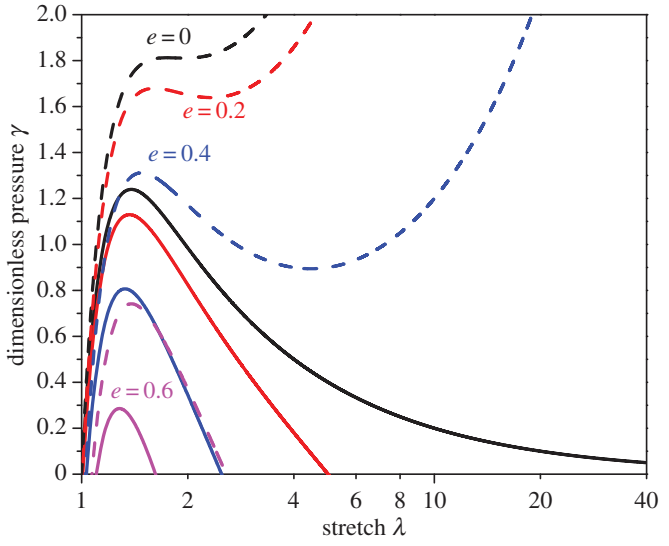

Figure 2. Variation of dimensionless inflation pressure γ with respect to the hoop stretch λ under a constant electric field in uniform inflation for neo-Hookean (continuous line) and Mooney–Rivlin with $\xi = 0.21$ (dashed line) models. (Online version in colour.)

in §3. From the present analysis, the pre-inflation pressure is found to have a remarkable effect on the pull-in instability parameters of the DE balloon in both the static and dynamic modes of operation, as shown in the upcoming discussion.

Firstly, we investigate the snap-through instability experienced by the DE balloon during inflation or under pressure control. The non-dimensional pressure (γ_c) and corresponding stretch (λ_p^c) at snap-through instability are extracted by solving the system of nonlinear algebraic equations (3.4) and (3.5). For neo-Hookean material model, we obtained the explicit expressions for critical dimensionless pressure and corresponding stretch as

$$\gamma^c = 1.2394 \quad \text{and} \quad \lambda_p^c = 1.3831. \tag{4.1}$$

Based on equilibrium equation (equation (3.4)), figure 2 plots the hoop stretch of DE balloon as a function of dimensionless internal pressure for four different non-dimensional electric fields, i.e. $e = 0, 0.2, 0.4$ and 0.6. The results for the neo-Hookean and the Mooney–Rivlin (with material constant $\xi = 0.21$) materials are represented by continuous and dashed lines, respectively. It is seen that the DE balloon expands with increase in the dimensionless pressure until a certain threshold pressure value. If the pressure is further increased, the balloon switches to a new stable state with sudden enhancement in its size because of the 'snap-through' phenomenon. This critical pressure (γ_c) reduces with increase in the electric field (e).

In this paper, for the parametric study on pull-in instability of the DE balloon, we consider four different cases having dimensionless pressure γ equal to 0, 0.3, 0.6 and 0.9 for the neo-Hookean and Mooney–Rivlin models, while for the Ogden model, γ is taken to be 0, 0.2, 0.4 and 0.6. Firstly, we adopted the neo-Hookean model of hyperelasticity for extracting pull-in parameters in both static and dynamic modes with the proposed approach. The nonlinear algebraic equations stated in equations (3.8)–(3.9) with aforementioned level of dimensionless pressure γ and material parameters $\alpha_1 = 2, \alpha_2 = 0$ and $\xi = 0$ are solved in MATLAB for extracting the static pull-in instability parameters of the DE balloon. The dimensionless static instability fields e_c and corresponding dimensionless actuation stretch $\lambda_{ac}^S = \lambda_c^S/\lambda_p$ for all the four cases are given in table 1. The numerical value of dynamic pull-in instability parameters e_c^D and $\lambda_{ac}^D = \lambda_c^D/\lambda_p$, i.e. instability electric field and corresponding actuation stretch, obtained by solving

Table 1. The pull-in instability parameters of a DE balloon actuator under consideration for four different values of dimensionless inflation pressure, with neo-Hookean and Mooney–Rivlin material models.

material model →	neo-Hookean				Mooney–Rivlin							
material parameters →	$\alpha_1 = 2,\ \alpha_2 = 0,\ \xi = 0$				$\alpha_1 = 2,\ \alpha_2 = -2,\ \xi = 0.1$ [52]				$\alpha_1 = 2,\ \alpha_2 = -2,\ \xi = 0.21$ [48]			
	static instability parameters		dynamic instability parameters		static instability parameters		dynamic instability parameters		static instability parameters		dynamic instability parameters	
dimensionless pressure (γ)	λ_{ac}^{S}	e_c^S	λ_{ac}^{D}	e_c^D	λ_{ac}^{S}	e_c^S	λ_{ac}^{D}	e_c^D	λ_{ac}^{S}	e_c^S	λ_{ac}^{D}	e_c^D
0.0	1.2599	0.6874	1.4656	0.6470	1.2847	0.7409	1.5170	0.7005	1.3113	0.7974	1.5735	0.7573
0.3	1.2460	0.5953	1.4375	0.5588	1.2756	0.6581	1.4990	0.6213	1.3067	0.7228	1.5656	0.6861
0.6	1.2253	0.4883	1.3959	0.4564	1.2627	0.5653	1.4732	0.5325	1.3008	0.6414	1.5553	0.6085
0.9	1.1890	0.3534	1.3246	0.3275	1.2424	0.4567	1.4327	0.4286	1.2924	0.5506	1.5408	0.5218

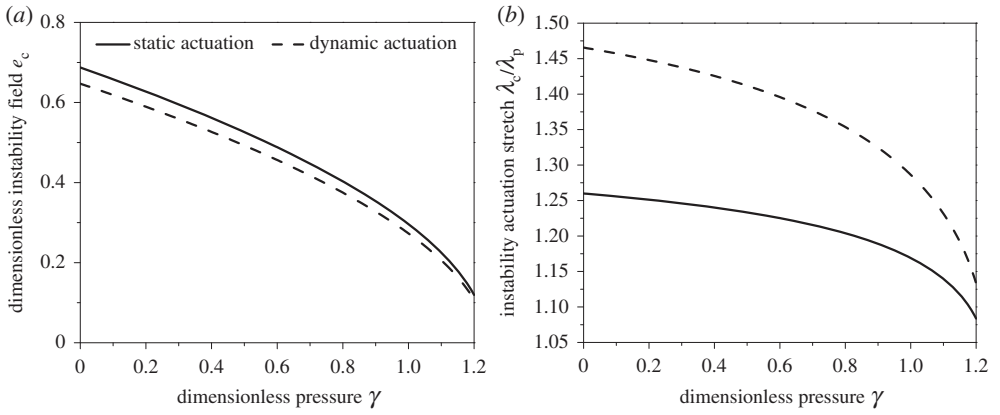

Figure 3. (*a*) The dimensionless instability electric field and (*b*) dimensionless instability actuation stretch, of the DE balloon as a function of dimensionless inflation pressure γ, for the neo-Hookean model.

nonlinear algebraic equations, i.e. equations (3.17)–(3.18), for the four different levels of non-dimensional pressure γ are also given in table 1. It is can be seen from the numerical values of the instability parameters listed in table 1 that, for the same level of pre-inflation pressure γ, the dynamic pull-in instability field is less than that corresponding to the static instability. Moreover, it also evident from numerical data that the critical actuation hoop stretch at the dynamic pull-in instability is remarkably more than that at the static pull-in. For the current model of hyperelasticity, the dimensionless instability parameters are independent of the material constants and are the function of dimensionless pressure γ only.

Figure 3 plots the non-dimensional static and dynamic pull-in instability parameters as a function of pre-inflation pressure. The variations for the static mode of operation are plotted using a continuous line, while that in dynamic operation are represented using a dashed line. From figure 3*a*, it can be inferred that the less electric field is required for triggering the pull-in instability, when the DE balloon is subjected to larger inflation pressure. Comparing the two curves in figure 3*a*, one can find that the dimensionless electric field required to trigger the dynamic pull-in instability is lower than that for the static instability at the same value of inflation pressure γ. Figure 3*b* demonstrates the variation of dynamic and static pull-in instability-induced actuation stretch ($\lambda_{ac} = \lambda_c/\lambda_p$) with the pre-inflating pressure. Figure 3*b* suggests that actuation stretch at instability decreases with increase in the dimensionless inflation pressure γ in both the modes of actuation. Furthermore, it is evident from figure 3*b* that at the same inflation pressure level γ, the actuation stretch (λ_a) experienced by the DE balloon actuator at the dynamic pull-in instability is much larger than that at the static pull-in instability.

Figure 4 plots the applied electric field (e) as a function of induced hoop stretch (λ) for three different levels of inflation pressure in both dynamic (denoted by the dashed lines) and static (continuous lines) modes. In this figure, the curves of static actuation are described by equation (3.8) expressed in a dimensionless form for the known value of γ, while the curves of dynamic actuation are described by equation (3.17). In case of dynamic actuation, the abscissa refers to the stretch amplitude of the oscillation cycle. The portion of curves left to the *X* belong to the stable branch, while the rest of the portion in the right of the cross symbol (*X*) represents the unstable branch. The respective branches for each value of γ meet at the bifurcation point, popularly referred to as the saddle-node bifurcation, as indicated in figure 4. It can be seen that the dynamic pull-in instability point lies at the intersection of the dynamic and static curves. This is because at the point of dynamic pull-in, the system is in the state of stagnation, characterized by zero acceleration and zero velocity.

Next, we consider a DE balloon made up of the Mooney–Rivlin-type materials and the instability parameters are extracted on the parallel lines discussed for the neo-Hookean model.

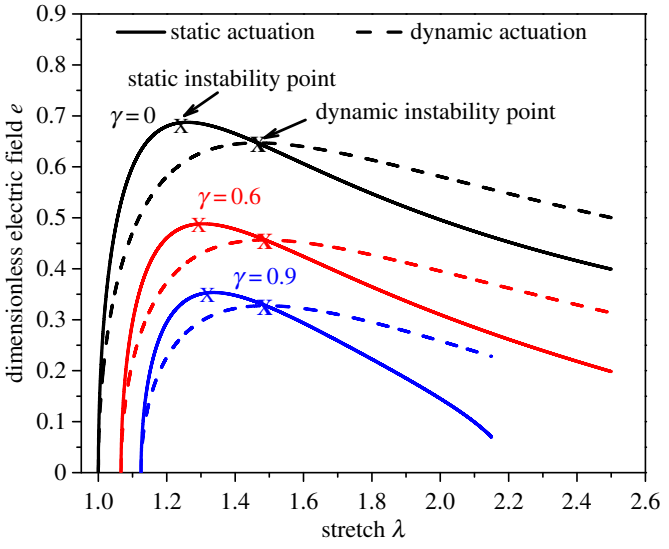

Figure 4. The non-dimensional electric field (e) as a function of hoop stretch (λ) of the DE balloon, for the neo-Hookean model at three different values of dimensionless pressure γ (0, 0.6 and 0.9), in static (continuous lines) and dynamic (dashed lines) modes. (Online version in colour.)

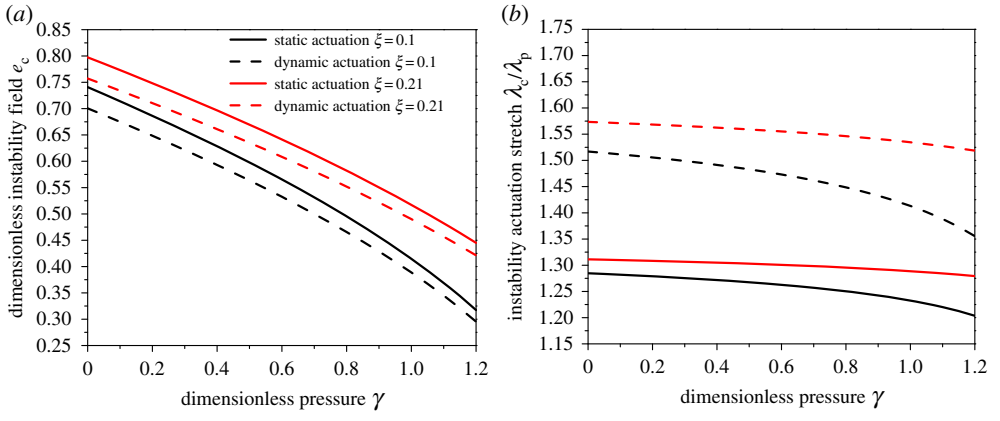

Figure 5. (*a*) The dimensionless instability electric field and (*b*) dimensionless instability actuation stretch, of the DE balloon as a function of dimensionless inflation pressure γ, for the Mooney–Rivlin model.

For the analysis, we choose two representative material parameters ($\xi = 0.1, 0.21$), which are also listed in table 1. These parameters are taken from references [48,52]. The estimates of dynamic and static pull-in instability parameters of the DE balloon for both the representative cases are illustrated in table 1 for the four different values of dimensionless pressure. For both the cases of Mooney–Rivlin model listed in table 1, the variation of the dimensionless pull-in instability field and corresponding dimensionless actuation stretch with dimensionless inflation pressure are depicted in figure 5*a*,*b*. These figures demonstrate the similar trends discussed for the neo-Hookean model in the foregoing discussion. From figure 5*a*,*b*, it is evident that the pull-in instability parameters depend on the material parameter ξ similar to the neo-Hookean model, in both of the actuation modes. For the same level of dimensionless pressure γ both the instability field and the instability actuation stretch increase as the value of material constant ξ increases.

Table 2. The pull-in instability parameters of the DE balloon actuator for different values of non-dimensional pressure with Ogden material model.

material parameters →	$\alpha_1 = 1.445, \alpha_2 = 4.248, \xi = 0.001$ [53]				$\alpha_1 = 1.130, \alpha_2 = 5.343, \xi = 0.00004$ [13]			
	static instability parameters		dynamic instability parameters		static instability parameters		dynamic instability parameters	
dimensionless pressure (γ)	λ_{ac}^{S}	e_c^S	λ_{ac}^{D}	e_c^D	λ_{ac}^{S}	e_c^S	λ_{ac}^{D}	e_c^D
0.0	1.2577	0.5946	1.4543	0.5581	1.2588	0.5292	1.4526	0.4962
0.2	1.2447	0.5240	1.4291	0.4902	1.2383	0.4486	1.4132	0.4190
0.4	1.2234	0.4435	1.3874	0.4135	1.2074	0.3520	1.3542	0.3266
0.6	1.1934	0.3466	1.3298	0.3209	1.1501	0.2193	1.2479	0.2006

Next, we consider the case of a DE balloon with the Ogden material model. The dimensionless pull-in instability parameters in the case of the Ogden model depend on the several material constants such as α_1, α_2 and ξ. For this material model, we take two representative cases, for which the material constants are adopted from the references [13,53]. The estimated critical values of static and dynamic pull-in parameters for both the representative cases of the DE balloon with four different values of non-dimensional pressure ($\gamma = 0$, 0.2, 0.4 and 0.6) are tabulated in table 2. Similar to the case of the neo-Hookean and Mooney–Rivlin models, it is observed from table 2 that the critical actuation stretch and electric field at instability in both the modes of actuation decrease with increasing value of γ. All the estimates discussed till this end in this section are obtained using the energy method.

Here, the corroboration of dynamic pull-in instability estimates obtained using the energy method for all material models under consideration is done by extracting the saddle-node bifurcation point in the transient response of hoop stretch achieved by numerically integrating the non-dimensional equation of motion given in equation (3.20) with the specific values of the material parameters. The plot in figure 6*a–c* depicts the dimensionless time of hoop stretch of the DE balloons made up of the neo-Hookean and Mooney–Rivlin with $\xi = 0.1$ and Ogden model with $\alpha_1 = 1.13$, $\alpha_2 = 5.343$ and $\xi = 0.00004$, respectively, for three different levels of pre-inflation pressure.

From the figure 6*a–c*, it is observed that the transient response of the DE balloon actuator for an applied electric field less than the electric field at the onset of dynamic instability is periodic. If the value of the applied electric field exceeds the critical electric field e_c^D, the time history response becomes non-periodic. However, by examining the figure 6*a–c*, one can infer that the dynamic pull-in instability parameters shown in tables 1 and 2 indeed correspond to the stagnation state of the DE balloon. This shows the utility of the energy method developed in the present paper. Figure 6*d* shows the response of the neo-Hookean type DE balloon on phase-plane plots. For different levels of the applied field at given value of dimensionless pressure, the non-periodic orbits are represented by a dashed lines, while the periodic orbits are depicted by the continuous lines. The important conclusions drawn from this investigation are summarized in the upcoming section.

5. Conclusion

In conclusion, we have outlined an energy-based method for estimating the dynamic pull-in instability parameters of the DE balloon actuator undergoing homogeneous deformation when subjected to pre-inflation pressure, and driven by a step voltage signal. We considered three material models of hyperelasticity, i.e. the Ogden model, Mooney–Rivlin model and neo-Hookean, for the analysis of electromechanical behaviour of the soft DE balloon. The pull-in parameters in the dynamic mode of actuation are extracted by setting the energy balance at the

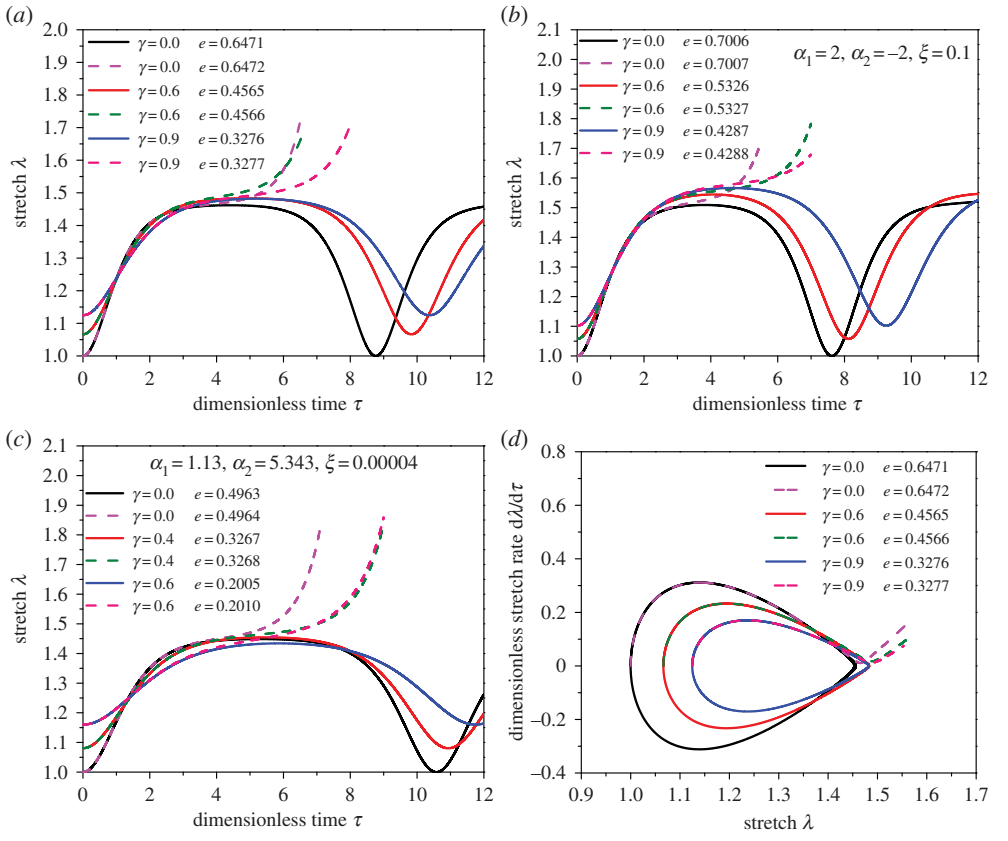

Figure 6. Dimensionless time evolution of hoop stretch for the (*a*) neo-Hookean, (*b*) Mooney–Rivlin, (*c*) Ogden models and (*d*) phase diagram for the neo-Hookean model, of the DE balloon with different levels of dimensionless pressure (γ) and electric fields (*e*). (Online version in colour.)

stagnation point in an oscillation cycle. The proposed method facilitates the accurate estimation of the dynamic pull-in parameters and evades the iterative method, examining the bifurcation points in the time history response of hoop stretch acquired by numerical integration of the equation of motion. The energy-based technique presented in this paper can be applied to the other DEAs and material models of interest.

A parametric study is performed for bringing out the influence of pre-inflation pressure on the static and dynamic pull-in parameters. The results indicate that the critical hoop stretch on the onset of dynamic instability is more than that corresponding to the static instability. For the neo-Hookean model, in particular, at zero pre-inflation pressure, the threshold hoop stretch corresponding to dynamic instability is approximately 116% of that at static instability. This difference reduces monotonically with increasing levels of pre-inflation pressure and finally diminishes at the limiting pressure γ^{c}. By contrast, a meagre difference is observed between the threshold electric fields sufficient for triggering the electromechanical instability in the static and dynamic modes of actuation. For the neo-Hookean model, at zero pre-inflation pressure, the electric field at static instability is 6.25% higher than that at dynamic instability, which reduces to zero at γ^{c}. For the other two material models (i.e. Mooney–Rivlin and Ogden), similar dependency of pull-in parameters on the pre-inflation pressure is observed; however, the exact values of instability parameters depend on the material constants. These inferences can find their potential use in designing the safe operating limits for the DE balloon actuators subjected to transient electric loads.

The present investigation has outlined an energy-based method for extracting the dynamic instability parameters of the DE balloons with constant inflation pressure. To highlight the method of solution, the discussion has been kept limited to the Ogden family of hyperelastic material models. In addition to extending its applicability to the other hyperelastic material models (Arruda–Boyce, Gent), the analysis can be refined to accommodate the effects of viscoelasticity.

Data accessibility. This article has no additional data.

Authors' contributions. All authors contributed equally in all aspects.

Competing interests. We have no competing interests.

Funding. This research is supported financially by the Science and Engineering Research Board, Government of India.

Acknowledgements. The authors gratefully acknowledge Dr D. M. Joglekar, DST-INSPIRE faculty, IIT Roorkee, for useful discussions during the development of the technique. The authors are also grateful to the anonymous reviewers for their valuable inputs.

References

1. Alexander H. 1971 Tensile instability of initially spherical balloons. *Int. J. Eng. Sci.* **9**, 151–160. (doi:10.1016/0020-7225(71)90017-6)
2. Green AE, Adkins JE. 1960 *Large elastic deformations and non-linear continuum mechanics*. Oxford, UK: Clarendon Press.
3. Haughton DM, Ogden RW. 1978 On the incremental equations in non-linear elasticity—II. Bifurcation of pressurized spherical shells. *J. Mech. Phys. Solids* **26**, 111–138. (doi:10.1016/0022-5096(78)90017-0)
4. Fu YB, Pearce SP, Liu KK. 2008 Post-bifurcation analysis of a thin-walled hyperelastic tube under inflation. *Int. J. Non Linear Mech.* **43**, 697–706. (doi:10.1016/j.ijnonlinmec.2008.03.003)
5. deBotton G, Bustamante R, Dorfmann A. 2013 Axisymmetric bifurcations of thick spherical shells under inflation and compression. *Int. J. Solids Struct.* **50**, 403–413. (doi:10.1016/j.ijsolstr.2012.10.004)
6. Wang T, Xu F, Huo Y, Potier-Ferry M. 2017 Snap-through instabilities of pressurized balloons: pear-shaped bifurcation and localized bulging. *Int. J. Non Linear Mech.* **98**, 137–144. (doi:10.1016/j.ijnonlinmec.2017.10.017)
7. Mangan R, Destrade M. 2015 Gent models for the inflation of spherical balloons. *Int. J. Non Linear Mech.* **68**, 52–58. Mechanics of Rubber - in Memory of Alan Gent.. (doi:10.1016/j.ijnonlinmec.2014.05.016)
8. Pelrine R, Kornbluh R, Pei Q, Joseph J. 2000 High-speed electrically actuated elastomers with strain greater than 100%. *Science* **287**, 836–839. (doi:10.1126/science.287.5454.836)
9. Carpi F, DeRossi D, Kornbluh R, Pelrine R, Sommer-Larsen P. 2008 *Dielectric elastomers as electromechanical transducers: fundamentals, materials, devices, models and applications of an emerging electroactive polymer technology*. Amsterdam, The Netherlands: Elsevier. doi:10.1016/B978-0-08-047488-5.X0001-9.
10. Wissler M, Mazza E. 2005 Modeling and simulation of dielectric elastomer actuators. *Smart Mater. Struct.* **14**, 1396–1402. (doi:10.1088/0964-1726/14/6/032)
11. Zhao X, Suo Z. 2007 Method to analyze electromechanical stability of dielectric elastomers. *Appl. Phys. Lett.* **91**, 061921. (doi:10.1063/1.2768641)
12. Zurlo G, Destrade M, DeTommasi D, Puglisi G. 2017 Catastrophic thinning of dielectric elastomers. *Phys. Rev. Lett.* **118**, 078001. (doi:10.1103/PhysRevLett.118.078001)
13. Kofod G. 2008 The static actuation of dielectric elastomer actuators: how does pre-stretch improve actuation?. *J. Phys. D: Appl. Phys.* **41**, 215405. (doi:10.1088/0022-3727/41/21/215405)
14. Berselli G, Vertechy R, Fontana M, Pellicciari M. 2014 An experimental assessment of the thermo-elastic response in acrylic elastomers and natural rubbers for application on electroactive polymer transducers. In *ASME 2014 Conf. on Smart Materials, Adaptive Structures and Intelligent Systems, Newport, RI, 8–10 September*, p. V001T03A027. New York, NY: American Society of Mechanical Engineers.
15. Jiménez SMA, McMeeking RM. 2013 Deformation dependent dielectric permittivity and its effect on actuator performance and stability. *Int. J. Non Linear Mech.* **57**, 183–191. (doi:10.1016/j.ijnonlinmec.2013.08.001)

16. Sharma AK, Bajpayee S, Joglekar DM, Joglekar MM. 2017 Dynamic instability of dielectric elastomer actuators subjected to unequal biaxial prestress. *Smart Mater. Struct.* **26**, 115019. (doi:10.1088/1361-665X/aa8923)
17. Artusi M, Potz M, Aristizabal J, Menon C, Cocuzza S, Debei S. 2011 Electroactive elastomeric actuators for the implementation of a deformable spherical rover. *IEEE. ASME. Trans. Mechatron.* **16**, 50–57. (doi:10.1109/TMECH.2010.2090163)
18. Soleimani M, Menon C. 2010 Preliminary investigation of a balloon-shape actuator based on electroactive elastomers. *Smart Mater. Struct.* **19**, 047001. (doi:10.1088/0964-1726/19/4/047001)
19. Ahmadi S, Gooyers M, Soleimani M, Menon C. 2013 Fabrication and electromechanical examination of a spherical dielectric elastomer actuator. *Smart Mater. Struct.* **22**, 115004. (doi:10.1088/0964-1726/22/11/115004)
20. Rudykh S, Bhattacharya K, de Botton G. 2012 Snap-through actuation of thick-wall electroactive balloons. *Int. J. Non Linear Mech.* **47**, 206–209. (doi:10.1016/j.ijnonlinmec.2011.05.006)
21. Fu YB, Xie YX. 2014 Stability of pear-shaped configurations bifurcated from a pressurized spherical balloon. *J. Mech. Phys. Solids* **68**, 33–44. (doi:10.1016/j.jmps.2014.03.007)
22. Xie YX, Liu JC, Fu YB. 2016 Bifurcation of a dielectric elastomer balloon under pressurized inflation and electric actuation. *Int. J. Solids Struct.* **78**, 182–188. (doi:10.1016/j.ijsolstr.2015.08.027)
23. Bortot E. 2017 Analysis of multilayer electro-active spherical balloons. *J. Mech. Phys. Solids* **101**, 250–267. (doi:10.1016/j.jmps.2017.02.001)
24. Liang X, Cai S. 2015 Shape bifurcation of a spherical dielectric elastomer balloon under the actions of internal pressure and electric voltage. *J. Appl. Mech.* **82**, 101002. (doi:10.1115/1.4030881)
25. Zhang H, Wang Y, Zhu J, Zhang Z. 2017 Balloon actuators based on the dielectric elastomer. In *IEEE International Conference on Industrial Technology* (*ICIT*), *2017, Toronto, Canada, 22–25 March*, pp. 654–658. New York, NY: IEEE.
26. Liang X, Cai S. 2017 New electromechanical instability modes in dielectric elastomer balloons. *Int. J. Solids Struct.* **132–133**, 96–104. (doi:10.1016/j.ijsolstr.2017.09.021)
27. Sun W, Wang H, Zhou J. 2015 Actuation and instability of interconnected dielectric elastomer balloons. *Appl. Phys. A* **119**, 443–449. (doi:10.1007/s00339-015-9001-y)
28. Zhu J, Cai S, Suo Z. 2010 Nonlinear oscillation of a dielectric elastomer balloon. *Polym. Int.* **59**, 378–383. (doi:10.1002/pi.2767)
29. Yong H, He X, Zhou Y. 2011 Dynamics of a thick-walled dielectric elastomer spherical shell. *Int. J. Eng. Sci.* **49**, 792–800. (doi:10.1016/j.ijengsci.2011.03.006)
30. Mockensturm EM, Goulbourne N. 2006 Dynamic response of dielectric elastomers. *Int. J. Non Linear Mech.* **41**, 388–395. (doi:10.1016/j.ijnonlinmec.2005.08.007)
31. Chen F, Zhu J, Wang MY. 2015 Dynamic electromechanical instability of a dielectric elastomer balloon. *EPL* (*Europhys. Lett.*) **112**, 47003. (doi:10.1209/0295-5075/112/47003)
32. Zhu J, Cai S, Suo Z. 2010 Resonant behavior of a membrane of a dielectric elastomer. *Int. J. Solids Struct.* **47**, 3254–3262. (doi:10.1016/j.ijsolstr.2010.08.008)
33. Dai H, Zou J, Wang L. 2016 Effect of initial stretch ratio on the electromechanical responses of dielectric elastomer actuators. *Appl. Phys. A* **122**, 1–6. (doi:10.1007/s00339-016-0046-3)
34. Wang J, Nguyen TD, Park HS. 2014 Electrostatically driven creep in viscoelastic dielectric elastomers. *J. Appl. Mech.* **81**, 051006. (doi:10.1115/1.4025999)
35. Eder-Goy D, Zhao Y, Xu BX. 2017 Dynamic pull-in instability of a prestretched viscous dielectric elastomer under electric loading. *Acta Mech.* **228**, 4293–4307. (doi:10.1007/s00707-017-1930-4)
36. Sheng J, Chen H, Li B, Wang Y. 2014 Nonlinear dynamic characteristics of a dielectric elastomer membrane undergoing in-plane deformation. *Smart Mater. Struct.* **23**, 045010. (doi:10.1088/0964-1726/23/4/045010)
37. Liu F, Zhou J. 2018 Shooting and arc-length continuation method for periodic solution and bifurcation of nonlinear oscillation of viscoelastic dielectric elastomers. *J. Appl. Mech.* **85**, 011005. (doi:10.1115/1.4038327)
38. Goulbourne N, Frecker M, Mockensturm E, Snyder A. 2003 Modeling of a dielectric elastomer diaphragm for a prosthetic blood pump. In *Proc. SPIE*, *San Diego, CA, 2–6 March*, vol. 5051, pp. 319–331. Wellingham, WA: International Society for Optics and Photonics.

39. Wang H, Cai S, Carpi F, Suo Z. 2012 Computational model of hydrostatically coupled dielectric elastomer actuators. *J. Appl. Mech.* **79**, 031008. (doi:10.1115/1.4005885)
40. Hochradel K, Rupitsch SJ, Sutor A, Lerch R, Vu DK, Steinmann P. 2012 Dynamic performance of dielectric elastomers utilized as acoustic actuators. *Appl. Phys. A* **107**, 531–538. (doi:10.1007/s00339-012-6837-2)
41. Keplinger C, Sun JY, Foo CC, Rothemund P, Whitesides GM, Suo Z. 2013 Stretchable, transparent, ionic conductors. *Science* **341**, 984–987. (doi:10.1126/science.1240228)
42. Xu BX, Mueller R, Theis A, Klassen M, Gross D. 2012 Dynamic analysis of dielectric elastomer actuators. *Appl. Phys. Lett.* **100**, 112903. (doi:10.1063/1.3694267)
43. Joglekar MM. 2014 An energy-based approach to extract the dynamic instability parameters of dielectric elastomer actuators. *J. Appl. Mech.* **81**, 091010. (doi:10.1115/1.4027925)
44. Joglekar MM. 2015 Dynamic instability parameters of dielectric elastomer actuators with equal biaxial prestress. *AIAA J.* **53**, 3129–3133. (doi:10.2514/1.J054062)
45. Ogden RW. 1972 Large deformation isotropic elasticity-on the correlation of theory and experiment for incompressible rubberlike solids. *Proc. R. Soc. Lond. A: Math. Phys. Eng. Sci.* **326**, 565–584. (doi:10.1098/rspa.1972.0026)
46. Patrick L, Gabor K, Silvain M. 2007 Characterization of dielectric elastomer actuators based on a hyperelastic film model. *Sens. Actuators A: Phys.* **135**, 748–757. (doi:10.1016/j.sna.2006.08.006)
47. Gu GY, Gupta U, Zhu J, Zhu LM, Zhu XY. 2015 Feedforward deformation control of a dielectric elastomer actuator based on a nonlinear dynamic model. *Appl. Phys. Lett.* **107**, 042907. (doi:10.1063/1.4927767)
48. Son S, Goulbourne N. 2010 Dynamic response of tubular dielectric elastomer transducers. *Int. J. Solids Struct.* **47**, 2672–2679. (doi:10.1016/j.ijsolstr.2010.05.019)
49. Weaver Jr W, Timoshenko SP, Young DH. 1990 *Vibration problems in engineering*. New York, NY: John Wiley & Sons.
50. Joglekar MM, Pawaskar DN. 2011 Estimation of oscillation period/switching time for electrostatically actuated microbeam type switches. *Int. J. Mech. Sci.* **53**, 116–125. (doi:10.1016/j.ijmecsci.2010.12.001)
51. Godara RK, Joglekar MM. 2015 Mitigation of residual oscillations in electrostatically actuated microbeams using a command-shaping approach. *J. Micromech. Microeng.* **25**, 115028. (doi:10.1088/0960-1317/25/11/115028)
52. Chakravarty UK, Albertani R. 2012 Experimental and finite element modal analysis of a pliant elastic membrane for micro air vehicles applications. *J. Appl. Mech.* **79**, 021004. (doi:10.1115/1.4005569)
53. Plante JS, Dubowsky S. 2006 Large-scale failure modes of dielectric elastomer actuators. *Int. J. Solids Struct.* **43**, 7727–7751. (doi:10.1016/j.ijsolstr.2006.03.026)